

Microwave and Infrared Scanning Radiometer Measurements of Air-Sea Temperature Difference in the Tropical Western Pacific

J. A. Shaw and J. H. Churnside
National Oceanic and Atmospheric Administration
Environmental Technology Laboratory
Boulder, Colorado

E. R. Westwater, Y. Han, V. Irisov, and H. Zorn
Cooperative Institute for Research in the Environmental Sciences
University of Colorado
National Oceanic and Atmospheric Administration
Environmental Technology Laboratory
Boulder, Colorado

D. Cimini
Department of Physics
University of L'Aquila
Coppito L'Aquila, Italy

Introduction

During June and July of 1999 we deployed a pair of scanning radiometers on the National Ocean and Atmospheric Administration (NOAA) R/V Ronald H. Brown (RHB) in the Tropical Western Pacific during the Nauru99 cruise, primarily in the vicinity of Nauru Island ($\sim 0^\circ$ latitude and 166° E longitude). This pair of vertically scanning microwave and infrared radiometers measures emission on the edge of a uniformly mixed atmospheric gas absorption line (O_2 for the mm-wave, and CO_2 for the IR). The horizontal atmospheric view is calibrated with a high-quality in situ temperature sensor. The AC-coupled radiometer output voltage generates air-sea temperature differences from the voltage difference between the horizontal and downward-looking vertical views. The same calibration uncertainty applies to both air and water measurements, so the differential temperature derived from the radiometer is more robust than subtracting two independent sensor readings. Furthermore, the radiometric signals relate to the important skin temperature rather than the bulk water temperature. Boundary-layer air temperature profiles can also be retrieved.

Scanning Microwave Radiometer

The 5-mm radiometer is designed for precise, continuous measurements of air-water temperature difference and for recovery of air temperature profiles (height from 0 m to 300 m) and was built by the

Lebedev Physical Institute of the Russian Academy of Sciences, Moscow, Russia. This device was first used from a research vessel during the Joint US-Russia Internal Waves Experiment (JUSREX) in July 1992 (Trokhimovski et al. 1998).

This technique measures oceanic and atmospheric emission in a wavelength band with relatively high atmospheric attenuation. We use the emission from the horizontal direction as a calibration point, since the brightness temperature (T_b) is essentially equal to the air temperature at the measurement height. The radiometer beam is scanned continuously in a vertical plane, and the radiometer measures T_b relative to the air temperature at the radiometer height.

The radiometer is a total power system with automatic compensation of the direct current in the output signal (a compensation-type radiometer). The radiometer employs no additional modulation, except for the antenna beam rotation at 1.3 Hz. A single frequency of 60.5 GHz is used with a total bandwidth of 4 GHz and a 3-dB beamwidth of 6° . The same measurements provide information about air temperature profiles in the lower atmosphere.

Scanning Infrared Radiometer

The scanning infrared radiometer was designed and built at NOAA Environmental Technology Laboratory. The wavelength band was chosen to have atmospheric weighting functions approximating those of the 5-mm radiometer. Thus, the atmospheric scans of the instruments should yield nearly identical angular emission, but the emission from the ocean surface would arise from an emissivity of nearly 0.98, in contrast to the 0.45 microwave emissivity. The infrared radiometer optical filter has a $14.2\ \mu\text{m}$ center wavelength and a $1.1\ \mu\text{m}$ bandpass, allowing the infrared radiometer to measure emission on the shortwave edge of a broad and highly opaque CO_2 absorption line. The incident emission from a 1° field of view is directed through the filter by the scanning mirror, and focused with an objective lens onto a photovoltaic HgCdTe detector cooled with liquid nitrogen. Both radiometers and the Vaisala HMP 233 temperature and humidity sensor were mounted on a boom that extended 5 m beyond the port side of the RHB. The height of the boom was 10 m above sea level (ASL). A picture of the deployments is shown in Figure 1.

Observations

Both radiometers scanned perpendicularly to the boom, but in opposite directions. The 5-mm radiometer rotated counter clockwise looking along the boom from the ship, and the infrared beam scanned clockwise. From Figure 1, it is apparent that some directions were blocked by the boom; at other angles, the radiometer saw structures not simply related to the ocean or atmosphere. However, in Figure 2, where relative T_b (without offset correction) is plotted as a function of angle, we see there is about 250° of the full scan from which we observe unobstructed signals from the sky or surface. Also shown in Figure 2 is a least-square fit to the atmospheric portion of the scan. An angle calibration was determined for each scan by setting the angle of minimum sky radiance to 90° , so that calibrated elevation angles are shown subsequently.



Figure 1. Boom-mounted radiometers and in situ sensors on the NOAA R/V Ronald H. Brown.

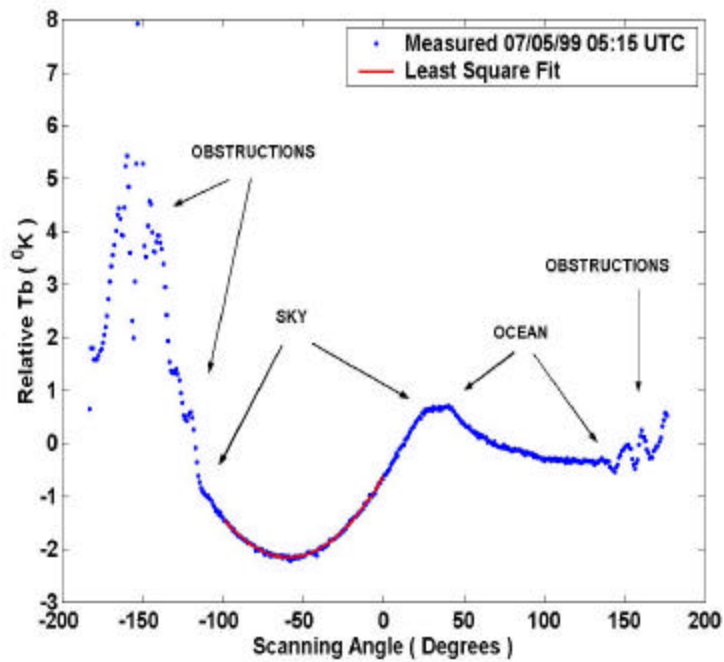


Figure 2. 5-mm radiometer signal, without offset correction, plotted versus uncalibrated scan angle.

Figure 3 shows calibrated Tbs from the 5-mm radiometer plotted vs. elevation angle for the unobstructed portion of the scan. In this figure, 90° is at zenith, and 180° is the unobstructed horizontal view. Angles larger than 180° correspond to the ocean view, while smaller angles correspond to the atmospheric view. In this figure, we have applied an angle calibration and we plot the vertical axis as Tb differences from zenith.

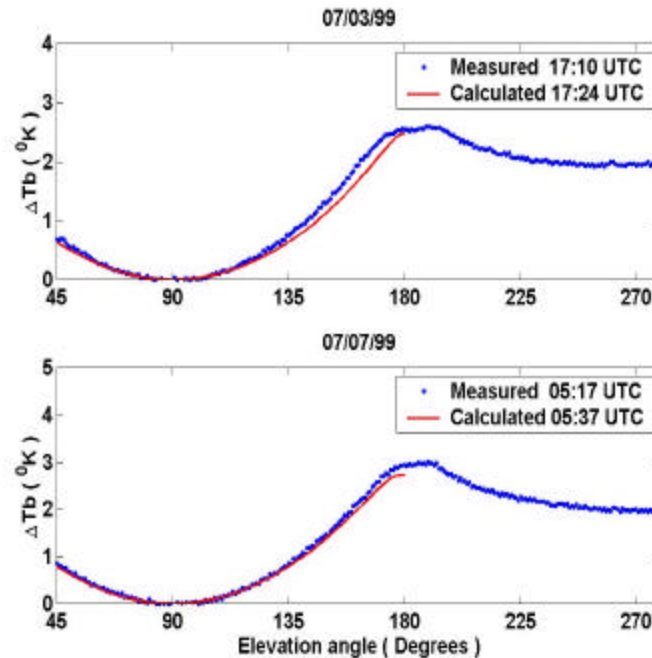


Figure 3. Tbs from the 5-mm radiometer, plotted versus elevation angle for the unobstructed portion of the scan. The measured data are 30-min averages, and the calculations are from radiosondes.

The measured data are 30-min averages, labeled by starting time. The calculations shown in this figure are made using atmospheric profiles from radiosondes launched on the ship at the noted time. Note that the scans shown here both exhibit maximum Tb at the horizontal view and minimum Tb at the zenith view because of the near lapse-rate atmospheric temperature profile. However, if this radiometer observes a low-level temperature inversion, the maximum brightness temperature shifts away from the horizontal.

Radiances from the atmospheric portion of the scan were converted into temperature profiles using a variation of linear statistical inversion. We used an a priori data set of radiosonde observations taken from previous ship-based observations in the Tropical Western Pacific, and calculated Tb as a function of elevation angle for each of the profiles. We next performed an Empirical Orthogonal Function (EOF) Decomposition to determine the most significant basis functions representing the a priori data set; only three functions were required to capture variations above the instrumental noise level of 0.2 K. Projection of the measured Tbs on the three EOFs, and the subsequent application of linear statistical inversion resulted in temperature profiles such as are shown in Figure 4. We estimate a retrieval accuracy of better than 0.2 K root mean square (rms) for altitudes less than 300 m.

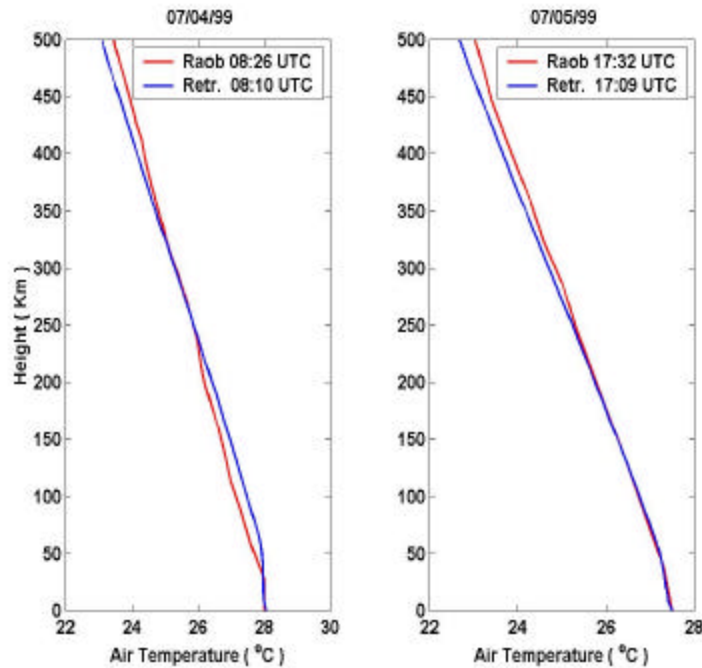


Figure 4. Atmospheric temperature profiles retrieved from the 5-mm radiometer (blue) and measured with radiosondes (red).

Figure 5 shows a 24-hour time series of air-sea temperature differences retrieved from the 5-mm radiometer (blue dots) and from in situ sensors (solid black line). The in situ data are differences between independent measurements from a floating sensor at about 5-cm depth and an air temperature sensor mounted on the mast of the RHB 15 m above the surface (Hare et al. 2000). The daytime data (~0-6 and 18-24 Universal Time Coordinates [UTC]) agree reasonably well, but the nighttime data (6 - 18 UTC) are significantly different. During the night, the air and water skin both cool, resulting in little change in the radiometrically derived temperature differences. However, the bulk water temperature stays relatively constant, leading to a changing air-water temperature difference. The magnitude of the difference we see between the bulk and skin measurements approaches 1K, which is consistent with other measurements during the same experiment.

Summary and Future Plans

The next step in this analysis is to compare air-sea temperature differences retrieved from the infrared and 5-mm radiometers. Note that the water skin depth is about 0.3 mm for the 5-mm instrument, and 0.01 mm for the infrared. It might be possible to examine small-scale skin-temperature gradients using these two radiometers together. Another potential product of this work is the microwave sea-surface emissivity, using the sea-surface temperature from the infrared radiometer.

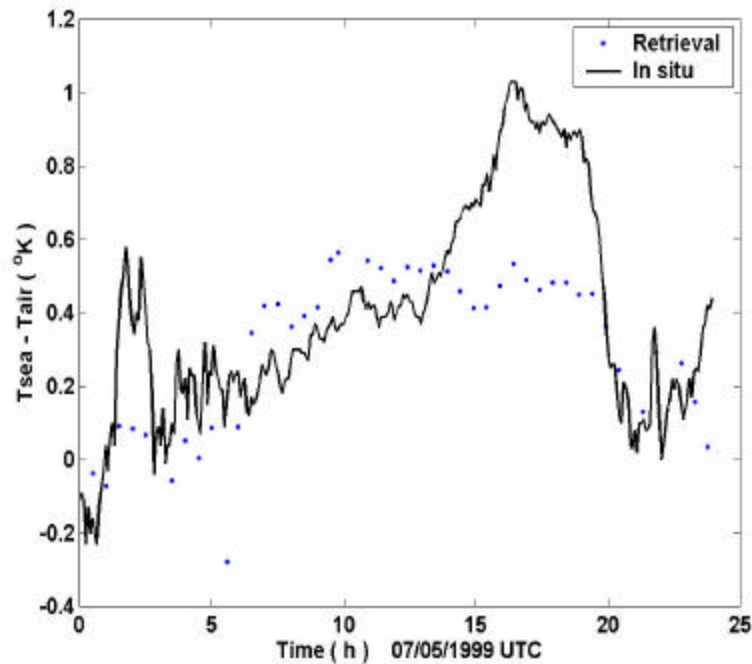


Figure 5. Air-sea temperature differences retrieved from the 5-mm radiometer (blue dots) and from in situ bulk air and water temperature sensors.

References

Hare, J. E., et al., 2000: Nauru99 ship and buoy intercomparison. This proceedings. Available URL: http://www.arm.gov/docs/documents/technical/conf_0003/hare-je.pdf

Trokhimovski, Y. G., E. R. Westwater, Y. Han, and V. Ye. Leuskiy, 1998: The results of air and sea surface temperature measurements using a 60 GHz microwave rotating radiometer. *IEEE Trans. Geoscience and Remote Sensing*, **36**, 3-15.